Relationship between Symmetry of Porphyrinic π-Conjugated Systems and Singlet Oxygen ($^1\Delta_g$) Yields: Low-Symmetry Tetraazaporphyrin Derivatives

Kazuyuki Ishii,[†] Hatsumi Itoya,[†] Hideya Miwa,[†] Mamoru Fujitsuka,[‡] Osamu Ito,[‡] and Nagao Kobayashi*,[†]

Department of Chemistry, Graduate School of Science, Tohoku University, Sendai 980-8578, Japan, and Institute of Multidisciplinary Research for Advanced Materials, Tohoku University, Sendai 980-8577, Japan

Received: January 6, 2005; In Final Form: April 18, 2005

We have investigated the excited-state properties and singlet oxygen ($^1\Delta_g$) generation mechanism in phthalocyanines (4M; M = H_2, Mg, or Zn) and in low-symmetry metal-free, magnesium, and zinc tetraazaporphyrins (TAPs), that is, monobenzo-substituted (1M), *adjacently* dibenzo-substituted (2AdM), *oppositely* dibenzo-substituted (2OpM), and tribenzo-substituted (3M) TAP derivatives, whose π conjugated systems were altered by fusing benzo rings. The S_{1x} and S_{1y} states (these lowest excited singlet states are degenerate in D_{4h} symmetry) split in the low-symmetry TAP derivatives. The excited-state energies were quantitatively determined from the electronic absorption spectra. The lowest excited triplet (T_{1x}) energies were also determined from phosphorescence spectra, while the second lowest excited triplet (T_{1y}) states were evaluated by using the energy splitting between the T_{1x} and T_{1y} states previously reported (Miwa, H.; Ishii, K.; Kobayashi, N. *Chem. Eur. J.* **2004**, *10*, 4422−4435). The singlet oxygen quantum yields (Φ_Δ) are strongly dependent on the π conjugated system. In particular, while the Φ_Δ value of $2AdH_2$ is smallest in our system, that of $2OpH_2$, an isomer of $2AdH_2$, is larger than that of 4Zn, in contrast to the heavy atom effect. The relationship between the molecular structure and Φ_Δ values can be transformed into a relationship between the $S_{1x} \rightarrow T_{1y}$ intersystem crossing rate constant (k_{ISC}) and the energy difference between the S_{1x} and T_{1y} states (ΔE_{SxTy}). In each of the Zn, Mg, and metal-free compounds, the Φ_Δ/τ_F values (τ_F: fluorescence lifetime), which are related to the k_{ISC} values, are proportional to $\exp(-\Delta E_{SxTy})$, indicating that singlet oxygen ($^1\Delta_g$) is produced via the T_{1y} state and that the $S_{1x} \rightarrow T_{1y}$ ISC process follows the energy-gap law. From the viewpoint of photodynamic therapy, our methodology, where the Φ_Δ value can be controlled by changing the symmetry of π conjugated systems without heavy elements, appears useful for preparing novel photosensitizers.

Introduction

Photodynamic therapy (PDT) is currently under intense study for the diagnosis, management, and treatment of various neoplasms on the basis of the combined use of selective uptake of photosensitizers into the malignant tissues and local irradiation of these with visible or near-infrared (NIR) light.[1−3] Most of the clinical experience has been obtained with Photofrin, which is a complex mixture comprising fractions of hematoporphyrin derivatives. Although Photofrin is effective in the treatment of several cancers, it has several disadvantages, such as a small extinction coefficient at the radiation wavelength (630 nm), as well as cutaneous phototoxicity over prolonged periods of time. These disadvantages have prompted a search for "second" and "third" generation photosensitizers, to achieve (1) high tumor to normal tissue accumulation ratios and (2) large extinction coefficients at longer wavelengths where light can penetrate skin.

To obtain intense absorption at longer wavelengths, various types of photosensitizers, including phthalocyanines (Pcs), naphthalocyanines, benzoporphins, purpurins, chlorins, porphycenes, pheophorbides, bacteriochlorins, and bacteriopheophorbides, have been investigated.[1−6] These compounds have intense absorption bands in the visible to near-IR regions, termed the Q-band, and may be divided into two groups by symmetry considerations. The first type is observed in Pc and naphthalocyanines with D_{4h} symmetry. In these systems, the LUMOs (e_{gx} and e_{gy}) are degenerate, so that an intense Q absorption band consisting of degenerate Q_x and Q_y bands occurs. On the other hand, split Q-bands are observed in benzoporphins, purpurins, chlorins, pheophorbides, bacteriochlorins, and bacteriopheophorbides because of lowering of the π-symmetry by reduction of the pyrrole rings or fusion of aromatic ring units onto the pyrrole rings. Since the breaking of the π-symmetry also brings about a red-shift of the Q-band, control of the π-symmetry is a promising method for preparing novel photosensitizers having strong absorption bands at longer wavelengths.

Singlet oxygen yield (Φ_Δ) is one of the most important parameters for PDT photosensitizers, since it is believed that PDT leading to biological damage usually involves the photochemical generation of singlet oxygen ($^1\Delta_g$) and the subsequent oxidation of tissues by direct attack on biological substrates. While the Φ_Δ values of several porphyrinic compounds have been reported,[7−11] any quantitative relationship between the symmetry of π-conjugated systems and Φ_Δ values has so far been unclear, in contrast to the well-characterized Q absorption bands.

Recently, we have examined a series of low-symmetry metallotetraazaporphyrin (MTAP; M = Zn and Pd) derivatives

* To whom correspondence should be addressed. E-mail: nagaok@mail.tains.tohoku.ac.jp.
[†] Department of Chemistry.
[‡] Institute of Multidisciplinary Research for Advanced Materials.

10.1021/jp050073a CCC: $30.25
Published on Web 06/15/2005

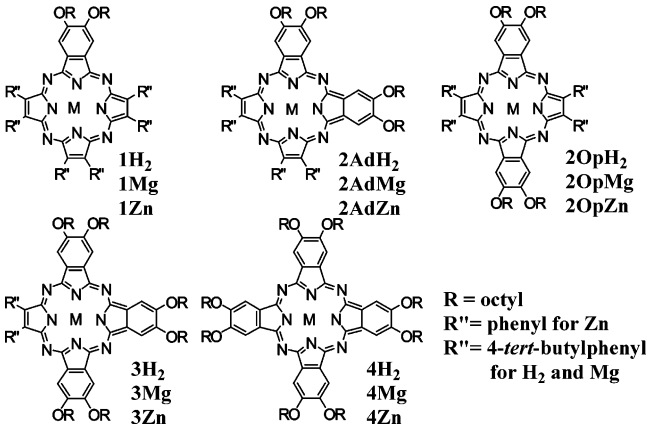

Figure 1. Molecular structures of low-symmetry TAP derivatives.

lying structurally between TAP and Pc, that is, monobenzo-, adjacently dibenzo-, oppositely dibenzo-, and tribenzo-substituted TAP derivatives (Scheme 1 in ref 12). In the case of our low-symmetry MTAP derivatives, the excited-state energies were quantitatively determined from the electronic absorption, magnetic circular dichroism (MCD), luminescence, and time-resolved EPR spectra (Figure 13 in ref 12). The ability to vary the excited states as required has motivated us, not only for controlling the excited-state dynamics and photochemical reaction yields by fusing benzo units, but also to elucidate the relationship between the symmetry of the porphyrinic π-conjugated system and the Φ_Δ values. In this study, we have investigated the excited-state properties and singlet oxygen ($^1\Delta_g$) generation mechanism in low-symmetry MTAP (M = H_2, Mg, and Zn) derivatives (Figure 1). Important features are as follows. (1) In metal-free and magnesium compounds, the excited-state energies are determined from electronic absorption and luminescence measurements. By comparing metal-free, Mg, and Zn compounds, the influence of the central element on the Φ_Δ value is examined. (2) The relationship between the Φ_Δ value and symmetry of the π-conjugated systems are investigated. This relationship is transformed into a quantitative relationship between the excited-state energies and excited-state dynamics, from which a universal rule for the singlet oxygen generation mechanism is proposed in relation to the porphyrinic π symmetry.

Experimental Section

Instrumental Techniques. Electronic absorption spectra were measured with a Hitachi U-3410 spectrophotometer. MCD measurements were made with a JASCO J-720 spectrodichrometer equipped with a JASCO electromagnet which produced magnetic fields of up to 1.09 T with parallel and antiparallel fields.[12] Fluorescence spectra were recorded at ambient temperature with a Hitachi F-4500 spectrofluorimeter. Fluorescence lifetimes were measured by a single-photon-counting method using an argon ion laser (Spectra-Physics, BeamLok 2060-10-SA), a pumped Ti:sapphire laser (Spectra-Physics, Tsunami 3950-L2S, 1.5 ps fwhm) with a pulse selector (Spectra-Physics, Model 3980), a second-harmonic generator (GWU-23PS), a picosecond light pulser (Hamamatsu Photonics PLP-02/041; 408 nm; 59-ps fwhm), and a streak-scope (Hamamatsu Photonics, C4334-02 or 01). NIR luminescence measurements were performed using a monochromator (JASCO CT-25CP) and a photomultiplier (Hamamatsu Photonics R5509-42), which was cooled at 193 K by a cold nitrogen gas flow system (Hamamatsu Photonics R6544-20).[11,12] The photon signals amplified by a fast preamplifier (Stanford Research SR445) were measured by the single-photon-counting method using a photon counter (Stanford Research SR400). A Nd:YAG laser (Spectra Physics INDI-30; 355 nm; 7-ns fwhm) or a dye laser (Sirah CSTR-LG532-TRI-T) pumped with a Nd:YAG laser (Spectra Physics INDI 40; 532 nm; 7-ns fwhm) was employed as an excitation source. As a solvent, spectral grade toluene (Nacalai Tesque Inc.) was used for all measurements (0.1−0.01 M pyridine was added for Zn and Mg complexes), while a 1:1 mixture of toluene and 1-iodoethane (Tokyo Chemical Industry Co, Ltd.) was employed for phosphorescence measurements.

Materials. Metal-free compounds were synthesized following the methods previously reported[12] and were characterized by electronic absorption and elemental analyses (Supporting Information). Magnesium complexes were synthesized by improving the method previously reported by Lindsey et al.[13] Typical experimental conditions for 1Mg are shown below.

[2²,2³-Dioctyloxybenzo[*b*]-7,8,12,13,17,18-hexa(*p*-*tert*-butylphenyl)-5,10,15, 20-tetraazaporphinato(2-)]magnesium(II), 1Mg. $1H_2$ (20 mg, 1.39×10^{-5} mol) and excess magnesium bromide diethyl etherate (700 mg, 2.72×10^{-3} mol) were refluxed in a toluene solution (16 mL) containing pyridine (80 μL) for 24 h. After adding toluene (50 mL), this organic solution was washed twice with 5% $NaHCO_3$ aqueous solution and was dried by Na_2SO_4. After evaporation of the solvent, the residue was purified by alumina and bio-beads gel (S-X1) columns using $CHCl_3$ as eluent. Recrystalization from $CHCl_3$/methanol produced 1Mg in 15% yield (2.8 mg).

1Mg; FAB mass (*m*/*z*): 1437 $[M + 1]^+$. Anal. Calcd for $C_{97}H_{118}N_8O_3Mg$: C, 79.34; H, 8.10; N, 7.58. Found: C, 78.381; H, 8.039; N, 7.554.

Similarly to 1Mg, the other magnesium complexes, 2AdMg, 2OpMg, 3Mg, and 4Mg, were synthesized from the corresponding metal-free compounds, respectively, and were characterized by electronic absorption, FAB-mass, ESI-TOF-mass, and elemental analyses (Supporting Information).

Results and Interpretations

Electronic Absorption Spectra. Electronic absorption spectra of magnesium complexes are shown in Figure 2 (left). In the electronic absorption spectrum of 4Mg, an intense Q band is seen at 683 nm, indicating that the S_{1x} and S_{1y} states are degenerate. On the other hand, the Q-bands split into the intense Q_y ($S_0 \rightarrow S_{1y}$ transition) and Q_x ($S_0 \rightarrow S_{1x}$ transition) bands for the low-symmetry TAP derivatives, 1Mg (C_{2v}; 632 and 675 nm) and 2OpMg (D_{2h}; 610 and 713 nm) (Figure 3). In the case of 3Mg, while three intense bands are observed at 634, 646, and 694 nm in the Q-band region, the bands at 646 and 694 nm were attributed to the Q_{y0-0} and Q_{x0-0} bands, respectively, by reference to 3Zn.[12] In the case of 2AdMg, a clear Q band splitting is not seen in the electronic absorption spectrum (660 nm). However, focusing on a weak shoulder at around 650 ∼ 660 nm, the Q-band splitting (=ΔE_{SS}) was evaluated as 260 cm^{-1} by band-deconvolution analyses, where the MCD bands of 2AdMg were fitted using two Faraday B terms of opposite sign.[12,14] The ΔE_{SS} value decreases in the order 2OpMg (2370 cm^{-1}) > 3Mg (1070 cm^{-1}) > 1Mg (1010 cm^{-1}) > 2AdMg (260 cm^{-1}), which is almost entirely similar to those of the corresponding Zn complexes. On the other hand, the Q-bands of the Mg complexes shift to the lower energy side compared with those of the corresponding zinc complexes (300 ∼ 400 cm^{-1}). These higher energy Q-bands of the Zn complexes are interpreted as due to destabilization of the LUMO and LUMO+1, as a result of an interaction between the π^* orbitals of the TAP ligand and the d_π orbitals of the Zn atom.[15]

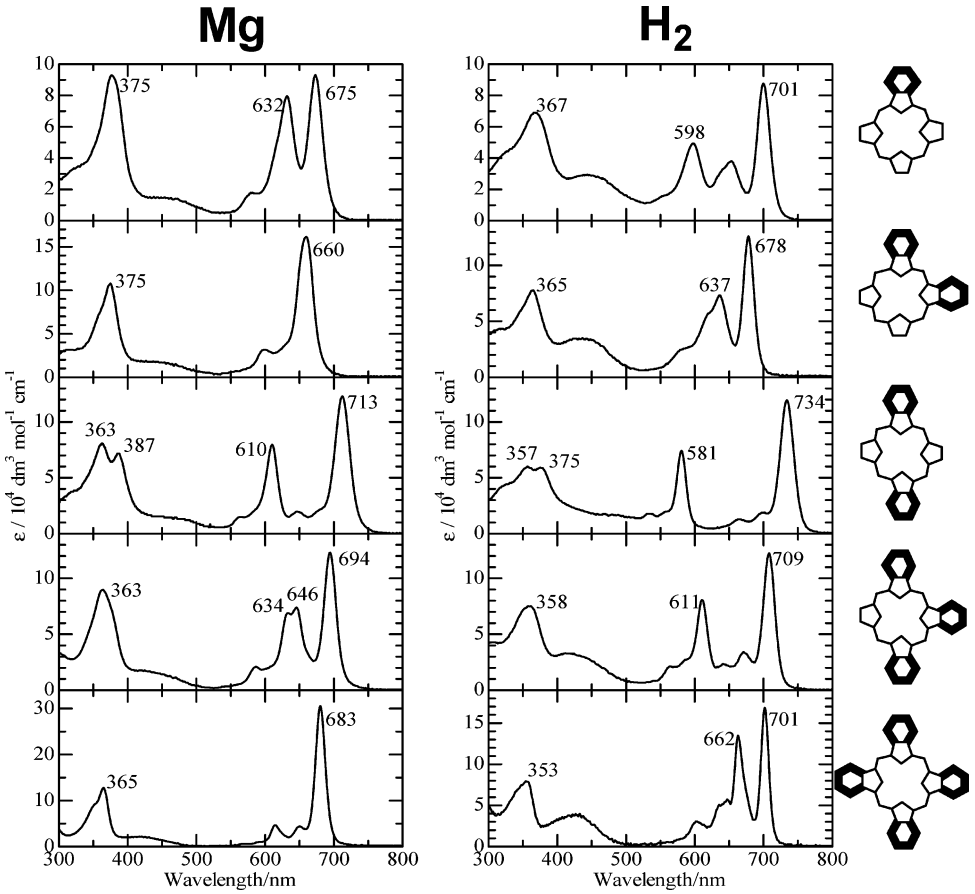

Figure 2. Electronic absorption spectra of Mg (left) and metal-free (right) compounds.

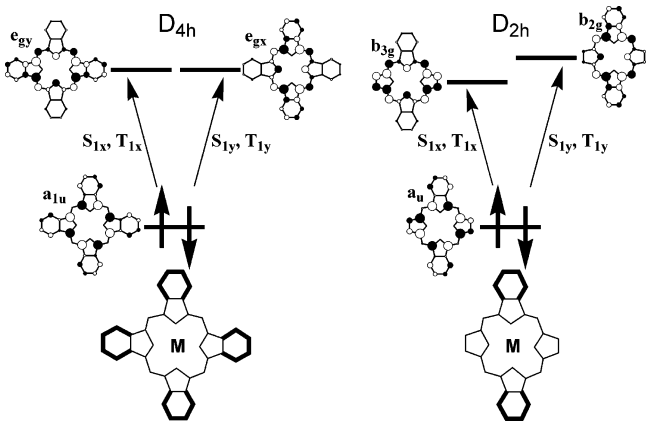

Figure 3. Excited-state properties of 4M and 2OpM.

Electronic absorption spectra of metal-free compounds are shown in Figure 2 (right). In the case of $4H_2$, the S_{1x} and S_{1y} states split, in contrast to 4Mg, as a result of the breaking of the D_{4h} symmetry because of the presence of the inner pyrrole protons.[15] In a similar manner, the substitutional change from Mg to 2H makes the Q-band splitting of low-symmetry TAP derivatives large. From the Q-band peaks, the ΔE_{SS} values of the metal-free compounds (ΔE_{SS}(Mf)) were determined to be 2450, 960, 3590, 2260, and 840 cm^{-1} for $1H_2$, $2AdH_2$, $2OpH_2$, $3H_2$, and $4H_2$, respectively, which are much larger than those of the corresponding Zn or Mg complexes.

Luminescence. All the Mg and metal-free derivatives show fluorescence at ambient temperature, as shown in Figure 4. Fluorescence lifetimes (τ_F) of the Mg complexes were estimated as 2.5, 3.8, 2.6, 3.4, and 6.5 ns for 1Mg, 2AdMg, 2OpMg, 3Mg, and 4Mg, respectively (Table 1). The τ_F value of 4Mg is longer than those of the other low-symmetry MgTAP derivatives. In the case of the Zn complexes, the τ_F values are shorter than those of the corresponding Mg complexes. Since the electronic absorption spectra of the Mg complexes are similar to those of the Zn complexes, the short τ_F values of the Zn complexes are interpreted due to spin−orbit coupling (SOC) on the zinc atom, which promotes intersystem crossing (ISC).[16,17] On the other hand, the τ_F values of the metal-free compounds were determined as 1.7, 0.081, 2.4, 4.2, and 6.1 ns, for $1H_2$, $2AdH_2$, $2OpH_2$, $3H_2$, and $4H_2$, respectively. The π symmetry dependence is larger in metal-free derivatives than in the Zn or Mg complexes.

TABLE 1: Fluorescence Lifetimes (τ_F) and Singlet Oxygen Yields (Φ_Δ)

compounds	τ_F/ns	Φ_Δ[a]	Φ_Δ/τ_F 10^{-8} s
1Zn	1.5	0.62	4.2
2AdZn	1.1	0.49	2.2
2OpZn	2.2	0.60	5.3
3Zn	1.5	0.55	3.6
4Zn	3.4	0.43	1.3
1Mg	2.5	0.27	1.1
2AdMg	3.8	0.18	0.48
2OpMg	2.6	0.24	0.91
3Mg	3.4	0.20	0.61
4Mg	6.5	0.14	0.21
$1H_2$	1.7	0.23	1.4
$2AdH_2$	0.081	0.010	1.3
$2OpH_2$	2.4	0.50	2.0
$3H_2$	4.2	0.27	0.64
$4H_2$	6.1	0.14	0.24

[a] Φ_Δ measurements were carried out with various laser powers, and the average Φ_Δ values were employed. The experimental errors were within 15%.

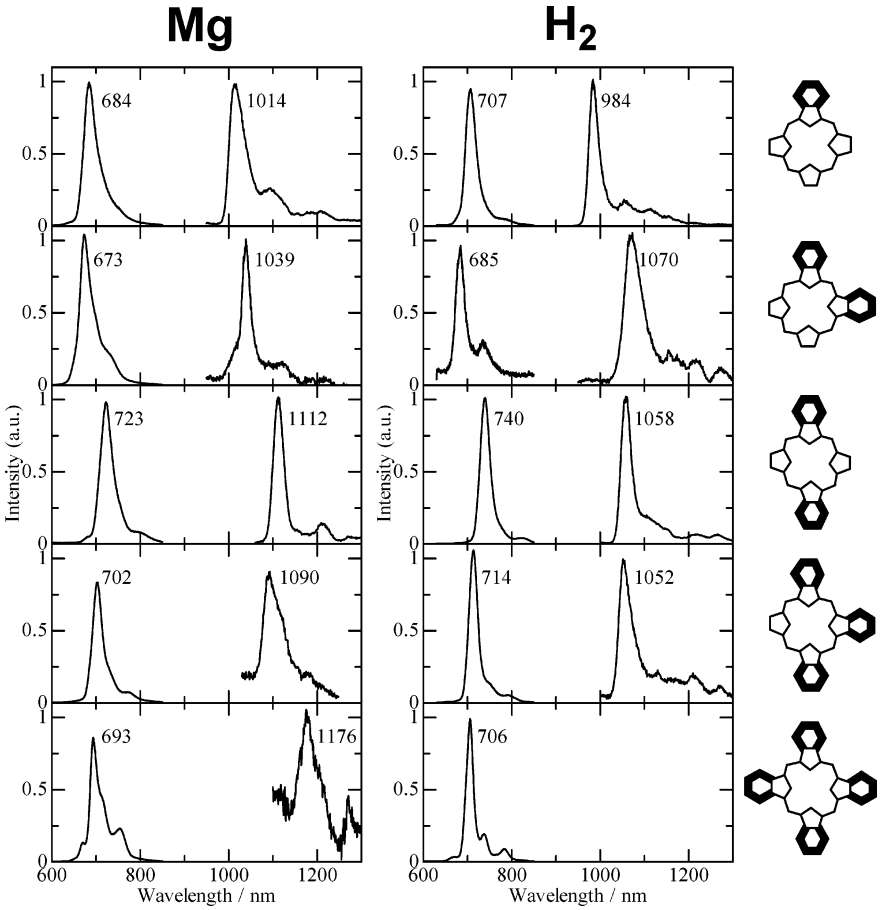

Figure 4. Luminescence spectra of Mg (left) and metal-free (right) compounds. The fluorescence and phosphorescence spectra were measured at ambient temperature and 77 K, respectively.

To determine the T_{1x} energies, phosphorescence measurements were carried out at 77 K. In the case of the Mg or metal-free TAP derivatives, only a few phosphorescence spectra have been previously reported because of the low phosphorescence efficiency.[17,18] To utilize heavy atom effects, a 1:1 mixture of toluene and 1-iodoethane (10^{-2} M pyridine was added for the Mg complexes) was employed as a solvent for the phosphorescence measurements.[16] Thus, we have succeeded in observing the phosphorescence spectra of Mg and metal-free compounds in the NIR region (Figure 4),[19,20] apart from $4H_2$. The T_{1x} energy of the Mg complexes decreases in the order 1Mg (1014 nm, 1.00×10^4 cm^{-1}) > 2AdMg (1039 nm, 9.62×10^3 cm^{-1}) > 3Mg (1090 nm, 9.17×10^3 cm^{-1}) > 2OpMg (1112 nm, 8.99×10^3 cm^{-1}) > 4Mg (1176 nm, 8.50×10^3 cm^{-1}), which is similar to the Zn complexes.[12] The phosphorescence peaks of the Mg complexes shift to lower energy compared with the corresponding Zn complexes, similarly to the Q absorption bands. In the case of the metal-free compounds, the T_{1x} energy decreases in the order $1H_2$ (984 nm, 1.02×10^4 cm^{-1}) > $3H_2$ (1052 nm, 9.51×10^3 cm^{-1}) > $2OpH_2$ (1058 nm, 9.45×10^3 cm^{-1}) > $2AdH_2$ (1070 nm, 9.35×10^3 cm^{-1}).

Singlet Oxygen Yield, Φ_Δ. The Φ_Δ values were investigated by monitoring the singlet oxygen ($^1\Delta_g$) luminescence at 1275 nm.[11,21,22] The values are summarized in Figure 5 and Table 1. In Figure 5, two important features are seen as follows.

(1) The Φ_Δ values of the Zn complexes are much larger than those of the corresponding Mg complexes, while the electronic structures are similar. This is reasonably interpreted by conventional SOC theory, called the heavy atom effect.[16−18]

(2) The Φ_Δ values strongly depend on the shape of the π conjugated system. In particular, the Φ_Δ dependence of the metal-free compounds is noteworthy. For example, while the Φ_Δ value of $2AdH_2$ is smallest in our system, that of $2OpH_2$ is larger than that of 4Zn, exceeding the heavy atom effect. That is, the Φ_Δ value increases with increasing splitting of the Q-band.

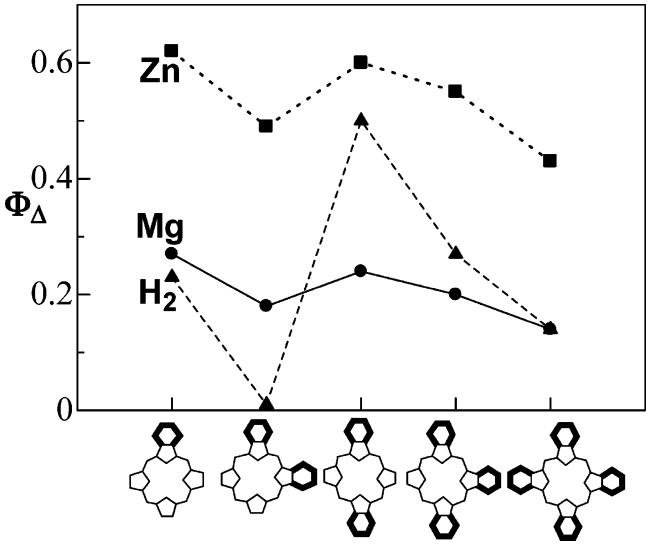

Figure 5. Relationships between the molecular structures and Φ_Δ values.

Thus, we have succeeded in changing the Φ_Δ value by fusing benzo units. These results will be analyzed in detail in the Discussion section.

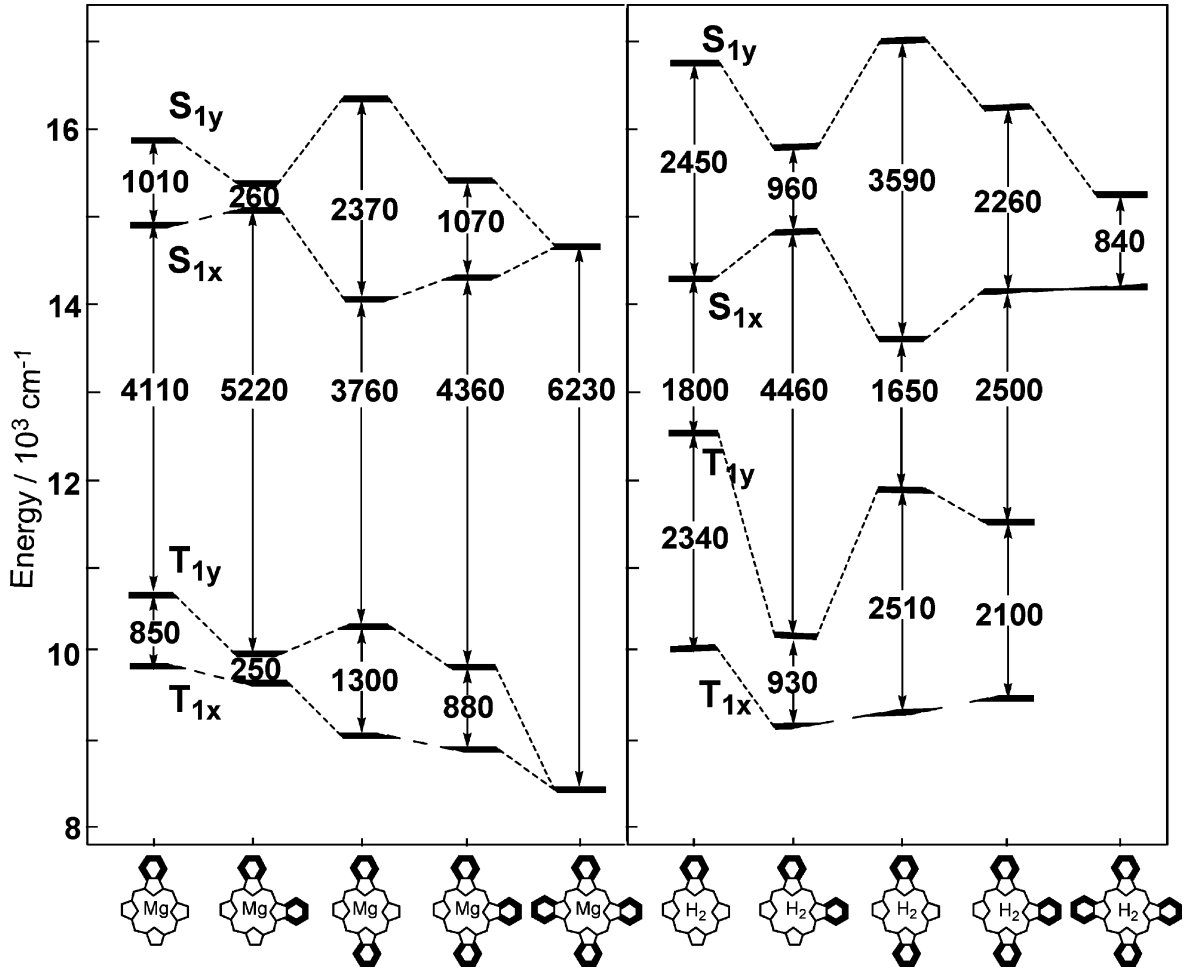

Figure 6. Summary of the ΔE_{SS} and ΔE_{TT} values of Mg (left) and metal-free (right) compounds.

Discussion

Excited-State Energies of Mg Complexes. The excited-state energies were quantitatively determined to clarify the singlet oxygen ($^1\Delta_g$) generation mechanism. In the case of the Mg complexes, the S_{1x} and S_{1y} energies were determined from the electronic absorption spectra, except for those of 2AdMg which were evaluated by band deconvolution analyses of the electronic absorption and MCD spectra.[12,14] The T_{1x} energies were determined from the position of phosphorescence peaks. The T_{1y} energies were evaluated by reference to the ΔE_{TT} values of Pd or Zn complexes (ΔE_{TT}: the energy splitting between the T_{1x} and T_{1y} states).[12] This approximation that the ΔE_{TT} values are similar among the Mg, Zn, and Pd complexes is plausible, since the magnitude of the Q-band splitting is similar for these complexes when comparing across complexes with the same π system.[12] The excited-state energies of our Mg complexes (Figure 6, left) are almost identical to those of the corresponding Zn complexes (Figure 13 in ref 12), indicating that a comparison between Zn and Mg complexes is appropriate for investigating the central metal effects.

Excited-State Energies of Metal-Free Compounds. In the case of the metal-free compounds, the S_{1x}, S_{1y}, and T_{1x} energies were determined from the electronic absorption and phosphorescence spectra. However, it is difficult to obtain the T_{1y} energies of metal-free compounds by directly utilizing the ΔE_{TT} values of the Pd or Zn complexes, since the Q-band splitting of metal-free compounds is different from those of the corresponding Zn or Pd complexes. To evaluate the ΔE_{TT} values of the metal-free compounds ($=\Delta E_{TT}(Mf)$), the $S_{1x}-S_{1y}$ splitting ($=\Delta E_{SS}(Mf)$) or the $\Delta E_{TT}(Mf)$ value is divided into two parts, as follows.

$$\Delta E_{SS}(Mf) = \Delta E_{SS}{}^{\pi} + \Delta E_{SS}{}^{2H} \quad (1a)$$

$$\Delta E_{TT}(Mf) = \Delta E_{TT}{}^{\pi} + \Delta E_{TT}{}^{2H} \quad (1b)$$

Here, the $S_{1x}-S_{1y}$ and $T_{1x}-T_{1y}$ splitting due to lowering of the π-symmetry of deprotonated dianionic species are termed $\Delta E_{SS}{}^{\pi}$ and $\Delta E_{TT}{}^{\pi}$, respectively, while those due to the inner pyrrole protons are termed $\Delta E_{SS}{}^{2H}$ and $\Delta E_{TT}{}^{2H}$, respectively. The ΔE_{SS} and ΔE_{TT} values of zinc complexes were employed as the $\Delta E_{SS}{}^{\pi}$ and $\Delta E_{TT}{}^{\pi}$ values, respectively, since the Q-band splitting is almost the same between the Mg, Zn, and Pd complexes. From the difference between the $\Delta E_{SS}(Mf)$ and $\Delta E_{SS}{}^{\pi}$ ($=\Delta E_{SS}(Zn)$) values, $\Delta E_{SS}{}^{2H}$ was evaluated as 1540, 680, 1200, 1200, and 800 cm^{-1}, for $1H_2$, $2AdH_2$, $2OpH_2$, $3H_2$, and $4H_2$, respectively. Here, we assumed $\Delta E_{SS}{}^{2H} \sim \Delta E_{TT}{}^{2H}$, since MO calculations indicate that the inner pyrrole protons barely change the π MO coefficients in the HOMO, LUMO, and LUMO+1, respectively.[23,24] Thus, the $\Delta E_{TT}(Mf)$ value was approximated according to the following equation.

$$\Delta E_{TT}(Mf) = \Delta E_{TT}{}^{\pi} + \Delta E_{SS}{}^{2H} = \Delta E_{TT}(Zn) + [\Delta E_{SS}(Mf) - \Delta E_{SS}(Zn)] \quad (2)$$

From eq 2, the excited-state energies of the metal-free com-

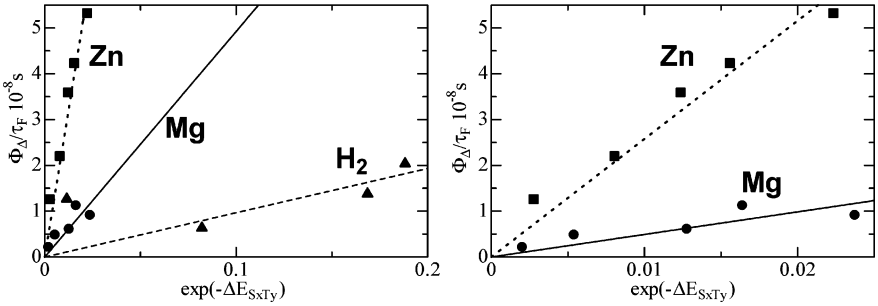

Figure 7. Relationships between the Φ_Δ/τ_F and $\exp(-\Delta E_{SxTy})$ values. The ΔE_{SxTy} value is in kcm^{-1}.

SCHEME 1: Singlet Oxygen ($^1\Delta_g$) Generation Mechanism in 4M and 2OpM.

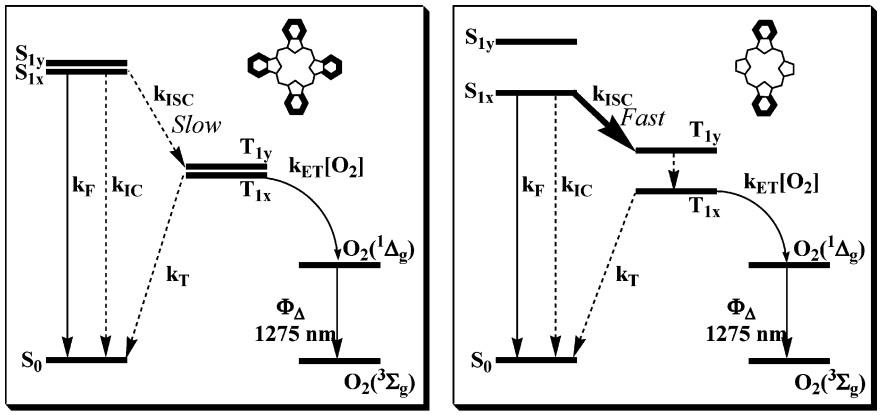

k_F: Fluorescence radiative decay rate constant
k_{IC}: Internal conversion rate constant
k_{ISC}: Intersystem crossing rate constant
k_T: Decay rate constant from the T_{1x} state
$k_{ET}[O_2]$: Energy transfer rate constant

pounds were evaluated as summarized in Figure 6 (right). The ΔE_{SS} and ΔE_{TT} values of the metal-free compounds are much larger than those of the zinc and magnesium complexes, because of the inner pyrrole protons.

Energy-Gap Law. By fusing the benzo units, we succeeded in controlling the Φ_Δ value. In particular, the Φ_Δ value of $2OpH_2$ was larger than that of 4Zn, while $2AdH_2$, being the isomer of $2OpH_2$, exhibited the smallest Φ_Δ value of our compounds. That is, the Φ_Δ value significantly depends on the symmetry of the porphyrinic π structure. To obtain a universal rule, the Φ_Δ values are now discussed quantitatively.

Since the singlet oxygen ($^1\Delta_g$) is generated via two processes, $S_1 \rightarrow T_1$ ISC of the photosensitizer and energy transfer from the T_1 photosensitizer to triplet oxygen ($^3\Sigma_g$), the Φ_Δ value is represented by $\Phi_{ET} \times \Phi_{ISC}$, where Φ_{ET} ($=k_{ET}[O_2]/(k_{ET}[O_2] + k_T)$) and Φ_{ISC} ($=k_{ISC}/(k_F + k_{IC} + k_{ISC})$) are the quantum yields of energy transfer and ISC, respectively (Scheme 1). Since the T_1 lifetimes of our Zn complexes are much longer than the energy transfer,[25−27] the energy-transfer efficiency is almost 100%, that is, $\Phi_\Delta \sim \Phi_{ISC}$, consistent with previous studies on Pc derivatives.[9,11] Thus, the $S_1 \rightarrow T_1$ ISC is the most important process in the relationship between the molecular structures and Φ_Δ values.

In the $S_1 \rightarrow T_1$ ISC, we focused on the ISC from the S_{1x} state to the T_{1y} state (Scheme 1). While the S_{1x} and S_{1y} states or the T_{1x} and T_{1y} states are almost entirely degenerate in the case of 4M and 2AdM, those of 1M, 2OpM, and 3M are split. As a result, the energy difference between the S_{1x} and T_{1y} states ($=\Delta E_{SxTy}$) is much smaller in 1M, 2OpM, and 3M than in 4M and 2AdM, enhancing the $S_{1x} \rightarrow T_{1y}$ ISC. Thus, we discuss the relationship between the $S_{1x} \rightarrow T_{1y}$ ISC and ΔE_{SxTy} value. The k_{ISC} value is represented using the wave functions of the S_{1x} ($=|\Phi_n^{Sx}\Phi_{es}^{Sx}>$) and T_{1y} ($=|\Phi_n^{Ty}\Phi_{es}^{Ty}>$) states as follows.[16]

$$k_{ISC} \propto |\langle \Phi_n^{Sx}|\Phi_n^{Ty}\rangle|^2 \times |\langle \Phi_{es}^{Sx}| H_{SOC} |\Phi_{es}^{Ty}\rangle|^2 \qquad (3)$$

Here, $|<\Phi_n^{Sx}|\Phi_n^{Ty}>|^2$ and $|<\Phi_{es}^{Sx}| H_{SOC} |\Phi_{es}^{Ty}>|^2$ denote the Franck−Condon factor and the SOC matrix element between the S_{1x} and T_{1y} states, respectively. The Franck−Condon factor correlates with the energy gap between the initial and final states, that is, $|<\Phi_n^{Sx}|\Phi_n^{Ty}>|^2 \propto \exp(-\Delta E_{SxTy})$.[16,28] Under this energy-gap law, the k_{ISC} value is represented as follows.

$$k_{ISC} = \alpha \times |\langle \Phi_{es}^{Sx}| H_{SOC} |\Phi_{es}^{Ty}\rangle|^2 \times \exp(-\Delta E_{SxTy}) \quad (4)$$

Experimental relationships between the Φ_Δ/τ_F ($\sim k_{ISC}$ when $\Phi_\Delta \sim \Phi_{ISC}$) and $\exp(-\Delta E_{SxTy})$ values are shown in Figure 7. In each of the Zn, Mg, and metal-free compounds, the Φ_Δ/τ_F values are proportional to $\exp(-\Delta E_{SxTy})$, indicating that singlet oxygen ($^1\Delta_g$) is produced via the T_{1y} state and that the $S_{1x} \rightarrow T_{1y}$ ISC process follows the energy-gap law. The slope increases in the order $H_2 < Mg < Zn$, consistent with conventional SOC theory.[16] In the case of the zinc complexes, many EPR results indicate that ISC from the S_{1x} state is selective to the *z* sublevel in the T_{1y} state, rather than the T_{1x} states, because of the *z* component of SOC between the d_{xz} and d_{yz} orbitals of the central zinc atom which are admixed with the LUMO and LUMO+1 of the TAP ligand, respectively.[12,17,29] Therefore, our experimental results for the Zn complexes, where singlet oxygen ($^1\Delta_g$) is produced via the T_{1y} state, is consistent with the previous EPR studies. On the other hand, in the case of the metal-free and Mg compounds, selective ISC to the *x* and *y* sublevels is

dominant because of the *x* and *y* components of SOC, which originate from the admixture of the S_1 (or T_1) state and the (σ,π^*) (or (π,σ^*)) configurations via vibronic coupling.[17,29] Thus, the selectivity between the T_{1x} and T_{1y} states had not been clarified. Therefore, these experimental relationships between the Φ_Δ/τ_F and $\exp(-\Delta E_{S_xT_y})$ values are the first experimental evidence of a $S_{1x} \rightarrow T_{1y}$ ISC process in metal-free and Mg compounds.

Conclusions

In this study, we have investigated the singlet oxygen ($^1\Delta_g$) generation mechanism, focusing on low-symmetry TAP derivatives. We have succeeded in increasing the Φ_Δ value by fusing benzo-units and have found a qualitative relationship, where the large Q-band splitting results in efficient generation of singlet oxygen ($^1\Delta_g$). Quantitative analyses on the excited-state energies show that the k_{ISC} value, being proportional to $\exp(-\Delta E_{S_xT_y})$, follows the energy-gap law. With respect to PDT, since heavy elements generally exhibit toxicity, our methodology, in which the Φ_Δ value can be controlled by the symmetry of the π conjugated system without heavy elements, should be useful for preparing novel photosensitizers.

Acknowledgment. This work was supported by a Grant-in-Aid for Young Scientists (Category A No. 14703007), Scientific Research in Priority Areas "Diagnosis and Treatment of Cancer" (No. 15025212 and 16023213), and the COE project, Giant Molecules and Complex Systems, 2004, from the Ministry of Education, Culture, Sports, Science, and Technology, Japan. Partial support from the Japan Society for the Promotion of Science, division 174, is also acknowledged.

Supporting Information Available: Electronic absorption and elemental analyses. This material is available free of charge via the Internet at http://pubs.acs.org.

References and Notes

(1) *Photodynamic Therapy*; Patrice, T., Ed.; The Royal Society of Chemistry: London, 2004.

(2) *Photodynamic Tumor Therapy: 2nd and 3rd Generation Photosensitizers*; Moser, J. G., Ed.; Harwood Academic Publishers: Amsterdam, 1998.

(3) *PDT Handbook: Advanced Technique of Photodynamic Therapy*; Kato, H., Okunaka, T., Eds.; Igaku-Shoin: Tokyo, 2002 (in Japanese).

(4) Rosenthal, I.; Ben-Hur, E. In *Phthalocyanines Properties and Applications*; Leznoff, C. C., Lever, A. B. P., Eds.; VCH Publishers: New York, 1989; Vol. I, pp 393−425.

(5) Rosenthal, I. In *Phthalocyanines Properties and Applications*; Leznoff, C. C., Lever, A. B. P., Eds.; VCH Publishers: New York, 1996; Vol. IV, pp 481−514.

(6) Pandey, R. K.; Zheng, G. In *The Porphyrin Handbook*; Kadish, K. M., Smith, K. M., Guilard, R., Eds.; Academic Press: San Diego, CA, 2000; Vol. 6, Chapter 43.

(7) Wilkinson, F.; Helman, W. P.; Ross, A. B. *J. Phys. Chem. Ref. Data* **1993**, *22*, 113.

(8) (a) Pineiro, M.; Carvalho, A. L.; Pereira, M. M.; Gonsalves, A. M. d'A. R.; Arnaut, L. G.; Formosinho, S. J. *Chem. Eur. J.* **1998**, *4*, 2299. (b) Pineiro, M.; Gonsalves, A. M. d'A. R.; Pereira, M. M.; Formosinho, S. J.; Arnaut, L. G. *J. Phys. Chem. A* **2002**, *106*, 3787. (c) Fukuzumi, S.; Ohkubo, K.; Chen, Y.; Pandey, R. K.; Zhan, R.; Shao, J.; Kadish, K. M. *J. Phys. Chem. A* **2002**, *106*, 5105.

(9) (a) Firey, P. A.; Ford, W. E.; Sounik, J. R.; Kenney, M. E.; Rodgers, M. A. J. *J. Am. Chem. Soc.* **1988**, *110*, 7626. (b) Aoudia, M.; Cheng, G.; Kennedy, V. O.; Kenney, M. E.; Rodgers, M. A. J. *J. Am. Chem. Soc.* **1997**, *119*, 6029.

(10) (a) Michelsen, U.; Kliesch, H.; Schnurpfeil, G.; Sobbi, A. K.; Whörle, D. *Photochem. Photobiol.* **1996**, *64*, 694. (b) Peeva, M.; Shopova, M.; Michelsen, U.; Wöhrle, D.; Petrov, G.; Diddens, H. *J. Porpyrins Phthalocyanines* **2001**, *5*, 645.

(11) Ishii, K.; Takeuchi, S.; Shimizu, S.; Kobayashi, N. *J. Am. Chem. Soc.* **2004**, *126*, 2082.

(12) Miwa, H.; Ishii, K.; Kobayashi, N. *Chem. Eur. J.* **2004**, *10*, 4422.

(13) Lindsey, J. S.; Woodford, J. N. *Inorg. Chem.* **1995**, *34*, 1063.

(14) Browett, W. R.; Stillman, M. J. *J. Comput. Chem.* **1987**, *11*, 241.

(15) (a) Gouterman, M. In *The Porphyrins*; Dolphin, D., Ed.; Academic Press: New York, 1978; Vol. 3, Chapter 1. (b) Stillman, M. J.; Nyokong, T. In *Phthalocyanines Properties and Applications*; Leznoff, C. C., Lever, A. B. P., Eds.; VCH Publishers: New York, 1989; Vol. I, Chapter 3. (c) Stillman, M. J. In *Phthalocyanines Properties and Applications*; Leznoff, C. C., Lever, A. B. P., Eds.; VCH Publishers: New York, 1993; Vol. III, Chapter 5.

(16) Turro, N. J. *Modern Molecular Photochemistry*; University Science Books: Mill Valley, California, 1991.

(17) Ishii, K.; Kobayashi, N. In *The Porphyrin Handbook*; Kadish, K. M., Smith, R. M., Guilard, R., Eds.; Academic Press: New York, 2003; Vol. 16, Chapter 102.

(18) (a) Vincett, P. S.; Voigt, E. M.; Rieckhoff, K. E. *J. Chem. Phys.* **1971**, *55*, 4131. (b) Dvornikov, S. S.; Knyukshto, V. N.; Kuzmitsky, V. A.; Shulga, A. M.; Solovyov, K. N. *J. Lumin.* **1981**, *23*, 373.

(19) Concentration dependence was examined for $1H_2$, 1Mg, 2OpMg, and 2AdMg. Phosphorescence peaks of $1H_2$, 1Mg, and 3Mg have minimum dependence on the concentration. In the case of 2AdMg, the main phosphorescence peak at 1039 nm was employed as the T_{1x} energy, while an additional phosphorescence peak appeared at around 1000 nm depending on the concentration.

(20) In the case of 3Mg, luminescence which may originate from decomposition becomes more intense at around 1100∼1200 nm with increasing laser irradiation time.

(21) In the Φ_Δ measurements, photon signals were counted at 4 μs (gate width = 5 μs) after 355-nm laser excitation to remove fluorescence influences. Shimizu, O.; Watanabe, J.; Imakubo, K.; Naito, S. *Chem. Lett.* **1999**, 67.

(22) The Φ_Δ values were determined by the use of benzophenone (=0.29). Gorman, A. A.; Hamblett, I.; Rodgers, M. A. J. *J. Am. Chem. Soc.* **1984**, *106*, 4679.

(23) Previous ZINDO/S calculations on the TAP derivatives indicate that the S_{1x} and S_{1y} states almost consist of the HOMO−LUMO and HOMO−LUMO+1 configurations, respectively.[12] In this case, the ΔE_{SS} value is represented by $[E_{LU+1} - \langle\phi_{HO}\phi_{LU+1}|\phi_{HO}\phi_{LU+1}\rangle + 2\langle\phi_{HO}\phi_{LU+1}|\phi_{LU+1}\phi_{HO}\rangle - \{E_{LU} - \langle\phi_{HO}\phi_{LU}|\phi_{HO}\phi_{LU}\rangle + 2\langle\phi_{HO}\phi_{LU}|\phi_{LU}\phi_{HO}\rangle\}]$ ($\langle\phi_i\phi_j|\phi_k\phi_l\rangle = \int\int\phi_i(1)\phi_j(2)e^2/r_{12}\phi_k(1)\phi_l(2)d\tau_1 d\tau_2$), where the E_i and ϕ_i denote the energy and wave function of *i* MO, respectively (HO = HOMO, LU = LUMO, LU+1 = LUMO+1). In a similar manner, the ΔE_{TT} value is represented by $[E_{LU+1} - \langle\phi_{HO}\phi_{LU+1}|\phi_{HO}\phi_{LU+1}\rangle - \{E_{LU} - \langle\phi_{HO}\phi_{LU}|\phi_{HO}\phi_{LU}\rangle\}]$. Thus, the difference between the $\Delta E_{SS}{}^{2H}$ and $\Delta E_{TT}{}^{2H}$ values is expressed by $[2\langle\phi_{HO}\phi_{LU+1}|\phi_{LU+1}\phi_{HO}\rangle - 2\langle\phi_{HO}\phi_{LU}|\phi_{LU}\phi_{HO}\rangle]$. Since the ZINDO/S MO calculations indicate that the π MO coefficients on the inner pyrrole protons of the HOMO, LUMO, and LUMO+1 MOs remain almost unchanged (Supporting Information),[24] our approximation that $\Delta E_{SS}{}^{2H} \sim \Delta E_{TT}{}^{2H}$ is plausible. Soares, L. de A., II; Trsic, M.; Berno, B.; Aroca, R. *Spectrochim. Acta, Part A* **1996**, *52*, 1245.

(24) MO calculations were performed within the framework of the ZINDO/S Hamiltonian.[12] (a) Ridley, J. E.; Zerner, M. C. *Theor. Chim. Acta* **1976**, *42*, 223. (b) Bacon, A. D.; Zerner, M. C. *Theor. Chim. Acta* **1979**, *53*, 21. (c) Anderson, W.; Edwards, W. D.; Zerner, M. C. *Inorg. Chem.* **1986**, *28*, 2728.

(25) Miwa, H. Dr Thesis, Tohoku University (in Japanese), 2001.

(26) Rodgers et al. have shown that the k_{ET} value depends on ΔG and is expressed by (1/9) $k_{diff}/[1 + \exp(\Delta G/RT)]$. Since $[1 + \exp(\Delta G/RT)] \sim 1$ in our system, the k_{ET} value was evaluated as $\sim 1.3 \times 10^9\ M^{-1}\ s^{-1}$, using $k_{diff} \sim 1.2 \times 10^{10}\ M^{-1}\ s^{-1}$ in toluene solution. Thus, the $k_{ET}[O_2]$ value was evaluated as $1.7 \times 10^6\ s^{-1}$ when $[O_2] = 1.3 \times 10^{-3}$ M.[27] Ford, W. E.; Rihter, B. D.; Rodgers, M. A. J.; Kenney, M. E. *J. Am. Chem. Soc.* **1989**, *111*, 2362.

(27) Wilhelm, E.; Battino, R. *Chem. Rev.* **1973**, *73*, 1.

(28) Robinson, G. W.; Frosch, R. P. *J. Chem. Phys.* **1963**, *38*, 1187.

(29) (a) van der Waals, J. H.; van Dorp, W. G.; Schaafsma, T. J. In *The Porphyrins*; Dolphin, D., Ed.; Academic Press: New York, 1978; Vol. 4, Chapter 3. (b) van Dorp, W. G.; Schoemaker, W. H.; Soma, M.; van der Waals, J. H. *Mol. Phys.* **1975**, *30*, 1701. (c) Ishii, K.; Ishizaki, T.; Kobayashi, N. *J. Phys. Chem. A* **1999**, *103*, 6060. (d) Ishii, K.; Abiko, S.; Kobayashi, N. *Inorg. Chem.* **2000**, *39*, 468. (e) Kobayashi, N.; Togashi, M.; Osa, T.; Ishii, K.; Yamauchi, S.; Hino, H. *J. Am. Chem. Soc.* **1996**, *118*, 1073. (f) Miwa, H.; Makarova, E. A.; Ishii, K.; Luk'yanets, E. A.; Kobayashi, N. *Chem. Eur. J.* **2002**, 1082. (g) Furuya, F.; Ishii, K.; Kobayashi, N. *J. Am. Chem. Soc.* **2002**, *124*, 12652.